

## Improving in-situ sound absorption measurements using sparse multichannel blind deconvolution

Bruno MASIERO<sup>(1)</sup>, Stelamaris Bertoli<sup>(2)</sup>, Alvaro Pais<sup>(3)</sup>

<sup>(1)</sup>Dept. of Communications, University of Campinas, Brazil, masiero@unicamp.br

<sup>(2)</sup>School of Civil Engineering, Architecture and Urban Design, Univ. of Campinas, Brazil, rolla@fec.unicamp.br

<sup>(3)</sup>School of Civil Engineering, Architecture and Urban Design, Univ. of Campinas, Brazil, aptdpais2@uem.br

### Abstract

The sound absorption of materials is traditionally measured in laboratory condition with one of two methods: random incidence in a reverberant chamber (ISO 354) or normal incidence in an impedance tube (ISO 10534). Nevertheless, there are some materials that cannot be measured in the lab, e.g., road surfaces, which are recommended to be measured in-situ with the use of a single microphone (ISO 13472). The latter method is based on time-windowing the measured impulse response to compare the incident and reflected wave components. Depending on the measurement setup, the size of the window may result in degraded measurement quality, specially at low frequencies. With the intention to alleviate this effect we evaluate three blind deconvolution approaches. These methods blindly estimates the response of the sound source, resulting in a cleaner (possibly more sparse) measurement that can than be used to estimate sound absorption. We compare the results of the aforementioned methods with free-field and averaged equalization for measurement at a wall covered with PET-wool. Even though the evaluated methods were able to “sharpen” the measured impulse responses, it showed no improvement in the calculation of the absorption coefficient.

Keywords: absorption coefficient, *in situ* measurement, sparse blind deconvolution.

### 1 INTRODUCTION

Environmental noise is harmful sound generated by human activities including road traffic, railways, air transport, industry, recreation and construction [1]. For instance, a survey applied in the Netherlands verified that road noise was rated as the most annoying source of noise (71%), followed by air traffic noise (13%) and neighbours’ noise (13%) [2]. Furthermore, long-term exposure to road traffic noise in association with air pollution is credited to accelerate neurocognitive decline and development of dementia [3]. Other studies indicate that transportation noise exposure may influence the occurrence of respiratory symptoms and exacerbate asthma in adults [4] and variation of blood pressure [5].

For the effective analysis of street noise attenuation, it is necessary to determine the sound absorption coefficient of the building walls. The determination of this coefficient is, commonly, made following two standards: ISO 354 (2003) method of determination of sound absorption coefficient in reverberant chamber and ISO 10534-1 (1996) method of determination of sound absorption coefficient in impedance tube. Both methods have some disadvantages. The impedance tube has limitations on sample area. For the desired frequency range from 250 Hz to 4000 Hz a sample with a diameter of only 10 cm is commonly used. In the reverberant chamber method, the samples must be installed on the chamber walls and this, for fixed systems, is impracticable. For these situations, in situ measurement techniques are an attractive alternative as they do not require a special environment to be set up.

*In situ* techniques can be used in both indoor and outdoor conditions. When conducting indoor in situ measurements the reverberation and sample size are of major concern, while the meteorological effects are of major concern in outdoor conditions. Brandão, Lenzi and Paul made a review of in situ impedance and sound absorption measurement techniques, arguing that the main method used in this cases is the temporal separation method. For this method, the challenge is to determine how the acoustic wave will behave in between the microphone and the sample under measurement [6].

Londhe, Rao and Blough [7] used the in situ method described in [8] to measure the sound absorption coefficient of grass. This method is based on the signal subtraction technique between the incident and reflected signals. Only one microphone and one sound source is needed for this method. When compared to the impedance tube the results have good agreement in the range between 400 Hz and 3000 Hz. Lacasta et al. used this same in situ method for modular greenery barriers and the results were equivalent to the results found in the literature [9]. Bustamante also performed the in situ technique on two materials: mineral wool and gypsum plaster board and concluded that the results were satisfactory [10].

The use of microphone arrays is one of the most recent approach to measure acoustic impedance in situ. It makes use of spatial filtering to separate the incident and the reflected components of the wave field close to the material under test. The simplest configurations use a linear array [11], while more complex configurations use planar [12] or spherical arrays [13].

All these microphone configurations use a loudspeaker as acoustic source to excite the system under measurement. Every such source has an uneven frequency response that translates to a time stretched impulse response which may result in the overlapping of incident and reflected components of the signal. Ideally, as we are interested on the ratio between reflected and direct sound, the influence of the loudspeaker should cancel out. However, the overlapping of the responses hinders this process, even after applying spatial filtering. In [10] the authors deconvolve the measured responses with a impulse response of the same loudspeaker measured in free-field and show considerable improvement with the single microphone method.

It may not always be the case that the free-field response of a loudspeaker is available for post-deconvolution or it may add unwanted noise in the deconvolution process. Therefore in this paper we evaluate the feasibility of applying blind deconvolution to eliminate the influence of the loudspeaker's response on the array measurement. We first present three such methods: prediction-error filters [14],  $\ell_p$ -norm sparse blind deconvolution [15] and sparse multichannel blind deconvolution [16]. We then evaluate the results of these three methods to a set of measurements with a four-microphone array conducted at the outside wall of a building covered with a commercially known material (PET-wool).

## 2 BLIND DECONVOLUTION

The topic of blind deconvolution has attracted the attention of the seismic community for several decades. In the following we present three methods derived for blind deconvolution under this context, but that can be directly applied to acoustics as well.

### 2.1 Prediction-error filters (PEF)

Given we have a sensor output signal  $x[n]$  of length  $N$ , the idea behind a prediction-error filter is to find a matched filter  $w[n]$  of length  $M \leq N$  that is capable of eliminating this signal or, equivalently,

$$e[j] = x[j] - \hat{x}[j] = x[j] - \sum_{i=1}^M x[j-i]w[i], \quad (1)$$

where  $e[j]$  is the residual error. Note that the sum in (1) is a convolution filter that estimates the value of  $x_j$  based on previous inputs,  $x_{j-i}$ ,  $i = 1, \dots, n_p$ . To avoid the trivial solution  $\mathbf{w} = \mathbf{0}$  we fix  $w[1] = 1$ . For the remaining values we define  $\mathbf{w} = [w[2] \ \dots \ w[M]]^T$  and calculate their values by minimizing the energy of the residual, i.e.,  $\|\mathbf{e}\|^2$ , which, according to [14], results in

$$\mathbf{w} = (\mathbf{X}^H \mathbf{X})^{-1} (-\mathbf{X}^H \mathbf{x}). \quad (2)$$

The matrix  $\mathbf{X}$  is the convolution matrix of  $\mathbf{x}$  concatenated with an extra first row of zeros. The PEF filter is the concatenation of  $w[1] = 1$  and the remaining element of  $\mathbf{w}$  calculated from (2).

### 2.2 $\ell_p$ -norm sparse blind deconvolution (LP-SBD)

The PEF framework has the drawback that it only works for minimum-phase systems, what is commonly not the case for loudspeakers. In order to alleviate the minimum-phase restriction the sparse blind deconvolution strategy was proposed in [15], where a deconvolution filter  $\mathbf{w}$  is estimated, much in the same sense as the PEF, but under sparse constraints. The authors argue that the  $\ell_p$ -norms can be seen as “contrast functions” for the blind deconvolution of sparse signals.

An input signal  $\mathbf{s}$  is convolved with the system impulse response  $\mathbf{h}$  (the Earth's impulse response for seismic applications) resulting in the sensor output signal  $\mathbf{x}$ . The objective of LP-SBD is to find a deconvolution filter  $\mathbf{w}$  whose output  $\mathbf{y}$  will recover the input signal  $\mathbf{s}$ , i.e.

$$\mathbf{y} = \mathbf{w} * \mathbf{x} = \mathbf{w} * \mathbf{h} * \mathbf{s} \equiv \mathbf{g} * \mathbf{s}. \quad (3)$$

The recovered signal should be a scaled and delayed version of the original signal, i.e.,  $y[n] = \alpha s[n-d]$ . Accordingly,  $\mathbf{g} = \mathbf{w} * \mathbf{h} = [0 \ \cdots \ 0 \ \alpha \ 0 \ \cdots \ 0]$ .

The LP-SBD is formulated as the following optimization problem

$$\begin{aligned} \underset{\mathbf{w}}{\text{minimize}} \quad & \|\mathbf{y}\|_p = \left( \sum_{i=0}^{N-1} \left| \sum_{k=0}^{L-1} w[k]x[i-k] \right|^p \right)^{1/p} \\ \text{subject to} \quad & \|\mathbf{g}\|_2 = 1. \end{aligned} \quad (4)$$

According to [15] the solution to this problem is equivalent to

$$\underset{\mathbf{w}}{\text{minimize}} \quad \frac{\|\mathbf{y}\|_p^p}{\|\mathbf{y}\|_2^p}, \quad (5)$$

and can be obtained with a gradient descent method applied to (5).

### 2.3 Sparse multichannel blind deconvolution (SMBD)

The LP-SBD algorithm incorporates assumptions on the structure of the signals' and the systems' impulse responses, assuming that the signal  $\mathbf{s}$  must be sparse. However, the LP-SBD does not take advantage of possible extra spatial information contained in the multichannel measurements. The SMBD does exactly that, still assuming that the original signals are sparse and incorporating a new assumption that the same system's impulse response is present in the same degree in all channels.

The data recorded by a sensor array with  $K$  sensors is modelled as

$$\mathbf{x}_k = \mathbf{h} * \mathbf{s}_k. \quad (6)$$

Note that each channel  $\mathbf{s}_k$  is convolved with the same system's impulse response  $\mathbf{h}$ . After applying the z-transform to equation (6) results in

$$X_k[z] = H[k]S_k[z]. \quad (7)$$

Noting that  $H[k]$  remains the same for every channel, we can recast (7) as

$$X_k[z]S_j[z] = X_j[z]S_k[z], \quad \forall k, j. \quad (8)$$

Multiplication in z-domain can be recast in time domain as the multiplication of  $\mathbf{X}$ —the convolution matrix of  $\mathbf{x}$ —and the signal vector  $\mathbf{s}$ , i.e.

$$\mathbf{X}_k \mathbf{s}_j - \mathbf{X}_j \mathbf{s}_k = \mathbf{0}, \quad (9)$$

leading to the homogeneous system of equations  $\mathbf{A}\mathbf{b} = \mathbf{0}$ , where

$$\mathbf{A} = \begin{bmatrix} \mathbf{X}_2 & -\mathbf{X}_1 & & & & \\ \mathbf{X}_3 & & -\mathbf{X}_1 & & & \\ \mathbf{X}_4 & & & -\mathbf{X}_1 & & \\ & \mathbf{X}_3 & -\mathbf{X}_2 & & & \\ & \mathbf{X}_4 & & -\mathbf{X}_2 & & \\ & & & & \ddots & \\ & & & & & \mathbf{X}_{K-1} & -\mathbf{X}_K \end{bmatrix} \quad \text{and} \quad \mathbf{b} = \begin{bmatrix} \mathbf{s}_1 \\ \mathbf{s}_2 \\ \vdots \\ \mathbf{s}_K \end{bmatrix}.$$

The above formulation ignored the presence of noise. If we consider noise the above formulation can be altered to  $\mathbf{A}\mathbf{b} = \mathbf{e}$ , where  $\mathbf{e}$  is the residual noise. In [16] it is assumed that  $\mathbf{e}$  is white and Gaussian which, they say, “is clearly a hypothesis that permits us to develop an algorithm, but one understands that  $\mathbf{e}$  is not necessarily white and Gaussian”.

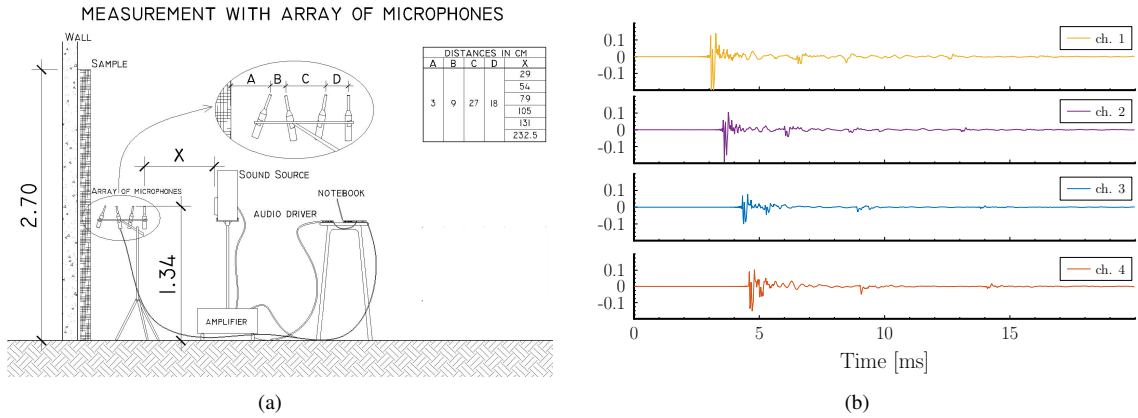


Figure 1. (a) Measurement setup of sound absorption coefficient using a microphone array. (b) Impulse response measured with loudspeaker placed 105 cm from the microphone array.

The “clean” signal  $\mathbf{s}$  is then extracted from the measured signal  $\mathbf{x}$  by minimizing the cost function

$$\hat{\mathbf{s}} = \arg \min_{\mathbf{x}} (\|\mathbf{A}\mathbf{b}\| + \lambda R(\mathbf{b})), \quad (10)$$

and

$$R(\mathbf{x}) = \sum_i \left( \sqrt{x_i^2 + \varepsilon^2} - \varepsilon \right) \quad (11)$$

where  $R(\mathbf{x})$  is a hybrid  $\ell_1/\ell_2$  regularization function used to promote sparsity, instead of the  $\ell_1$ -norm, as it is differentiable, allowing a simpler solution to the optimization procedure [16]. To avoid the trivial solution the restriction  $\mathbf{b}^H \mathbf{b} = 1$  is added.

While the PEF and LP-SBD formulations provide a linear filter that is applied to all channel data to eliminate the influence of a common impulse response resulting in a set of “clean” signals, the SMBD gives the “clean” signals directly as a result of its non-linear minimization procedure. For that reason, the SMBD gives no warranty that the spectral characteristics of the signals will be only globally altered.

### 3 EXPERIMENTAL SETUP

To evaluate the above mentioned algorithms we use a set of array measurements originally conducted to compare single channel measurement and array measurements to calculate the absorption coefficient of a material under test [17]. The examples shown in next section used a PET wool manufactured by Trisoft. The width of the material is 25 mm and each module has  $1.00 \text{ m} \times 1.00 \text{ m}$ . For the measurement, an external wall was covered with nine modules of the material, covering a total area of  $3.00 \text{ m} \times 3.00 \text{ m}$ . The superficial density is  $0.7 \text{ kg/m}^2$ . As expected of fibrous material, the high absorption performance is in high frequencies. In this work, the sound source used was a custom made loudspeaker with a coaxial driver model F6 from maker Bravox, the amplifier was a B&K model 2716, the microphones were Behringer ECM 8000, and the audio interface was a Presonus AudioBox USB. The signal processing was made in MatLab with the freely available ITA toolbox<sup>1</sup>. The excitation signal used for the test was a logarithmic sweep with duration of 6 s and frequency range from 20 Hz to 20 kHz. The position of microphones and sound source in relation to the material under test is described in Fig. 1(a). The array had a non-redundant geometry [18] and we evaluated several source distances.

As a reference, we compare the results with the measurement of sound absorption coefficient made with a commercial impedance tube from maker BSWA.

<sup>1</sup>[www.ita-toolbox.org](http://www.ita-toolbox.org)

## 4 RESULTS

We applied the methods discussed in section 2 at the impulse responses obtained with the setup presented in the previous section to eliminate the influence of the loudspeaker's impulse response on the measurements. We compare the result of these three methods (EP, LP-SBD, and SMBD) with three other approaches: inverse filtering with 1) the loudspeaker's impulse response measured at an open space, 2) the average of the aligned impulse responses of each channel, and 3) the median of the time samples of the aligned responses of each channel.

We observed that all these methods work very well with synthetic signals. In this manuscript we restrict ourselves to measured signals. We show in Fig. 1(b) the impulse responses measured with the array geometry presented in Fig. 1(a) at a source distance of 105 cm. Analysing the response in channel 1 we can observe that the loudspeaker's response (direct sound) has not yet faded away when the first reflection (reflected sound) arrives. At channel 4 (microphone closes to the wall) it is not possible anymore to tell both components apart. That is, if we simply apply the single microphone with time windows describe in [8] we would window out a significant part of the system's impulse response.

As proposed in [10], we approximated the loudspeaker's free-field response by measuring it facing against the wall and equalized the measurement with the inverse of the free-field response. The results in Fig. 2(a) show that both the direct and the reflected components are now more compact, however a considerable amount of noise was introduced in the process. Another strategy is to use the fact that we have an array measurement and average the time aligned signals to estimate the common component of all signals. This is equivalent to a delay-and-sum beamformer pointed at the direction of the source [19]. We observe in Fig. 2(b) that the components are compact and the signals show less noise than the free-field attempt. However, several new impulses appear in between the two main components caused by the presence of attenuated versions of the reflection in the average signal. To eliminate this effect we substitute the mean function by the median function, which is less sensitive to outliers. The signal equalized in this manner, shown in Fig. 2(c), do not show the presence of these unwanted spikes between the two components of interest.

The equalization methods discussed so far result in noisy signals that result in noisy estimates of the absorption coefficient (see Fig. 3). This is the reason why we investigate other methods to eliminate the system's response and, ideally, also reduce measurement noise. As can be seen in Fig. 2(d), the PEF failed in this task, what could be expected as loudspeakers usually cannot be described as minimum-phase systems. The LP-SBD does a much better job in finding a linear filter to eliminate the system's response, as can be seen in Fig. 2(e). Note that the results with LP-SBD are strongly dependent on the choice of  $p$ ; for this example we chose  $p = 4$ , which showed better results after trial-and-error tuning process. Regardless of the choice of  $p$ , however, we observed that the LP-SBD still shows a considerable amount of residual noise. The final algorithm to be evaluated was the SMBD. This algorithm now requires the tuning of two parameters:  $\epsilon$  and  $\lambda$ . The smaller the  $\epsilon$ , the closer  $R(\mathbf{x})$  resembles the  $\ell_1$ -norm and thus the more it sparsifies the result. On the other hand, the larger the value of  $\lambda$ , the more  $R(\mathbf{x})$  influences the optimization and, again, the more it sparsifies the result. After a trial-and-error tuning procedure we obtained the results in Fig. 2(f), which is very compact shows little residual noise.

These results suggest that the SMBD is a very promising pre-processing for the later extraction of the absorption coefficient. However, as can be seen in Fig. 3, the calculation with LP-BSD and SMBD cannot be regarded in anyway as better than the calculations with the first three methods, even though the SMBD did somehow reduce the oscillations in low frequency bands. Furthermore, if we set  $\lambda$  to high, the algorithm will be forcing too much sparsity, which may, at last, hamper the proper recovery of the reflection component (as it is a low pass filtered impulse and, thus, time spread). If that happens, we loose information in the low frequencies of the reflected component and the resulting absorption coefficient is much flatter, however possibly incorrect, in the lower frequency bands.

## 5 FINAL REMARKS

We evaluated three different blind deconvolution methods in order to extract the influence of the system's response (in our case the loudspeaker) in an array measurement and compared their results with an equalization based on a free-field measurement of the loudspeaker's response and a spatial filtered version of the array measurement response.

We verified that the PEF was not able to eliminate the system's response while both sparsity based techniques

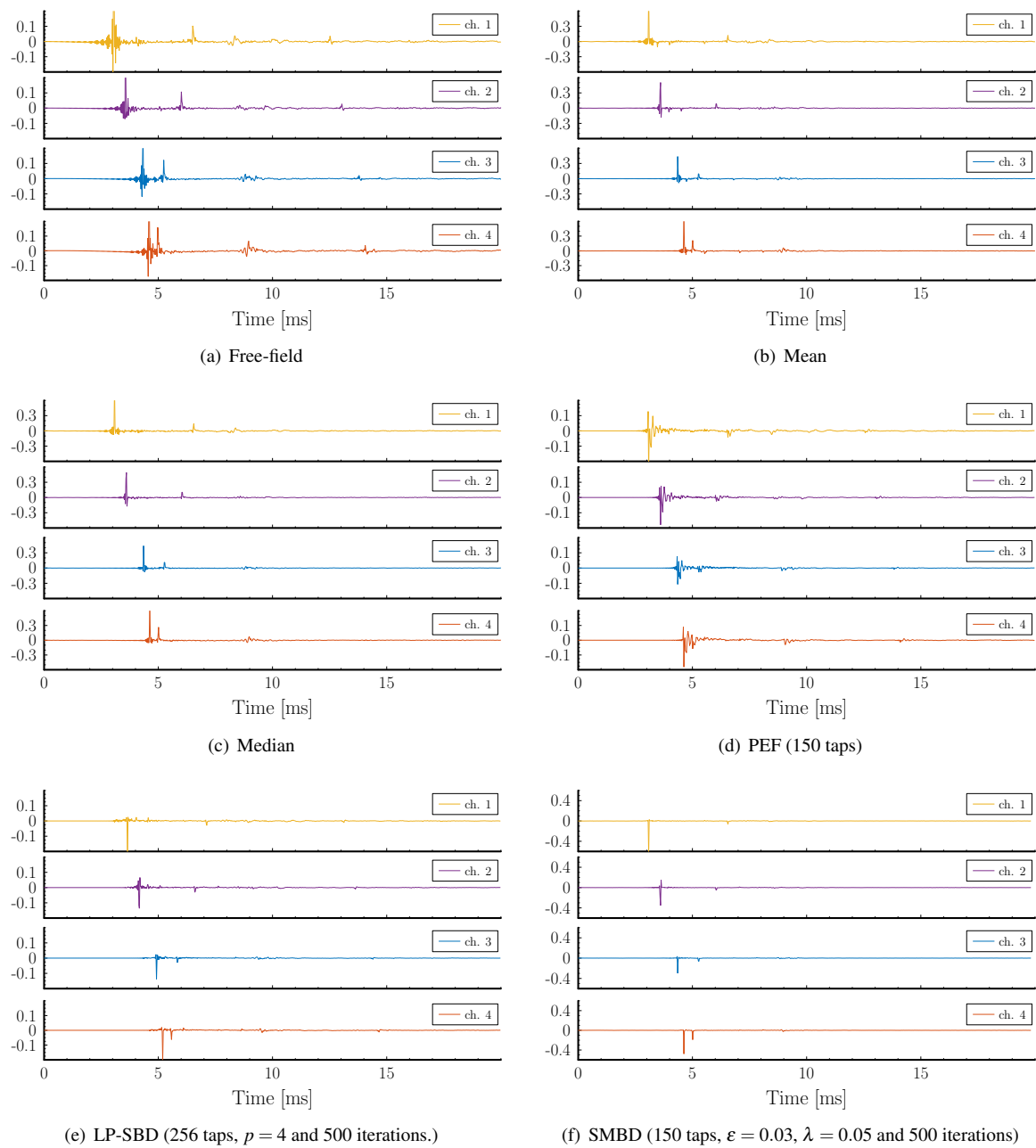


Figure 2. Equalized array impulse responses after the original signal from Fig. 1(b) was equalized with six different blind and non-blind deconvolution methods.

were successful in doing so. The LP-SBD, based on linear filtering resulted in large residual noise while the non-linear SMBD method resulted in very sharp impulse responses with little additive noise. Nevertheless, we could see no improvement in the calculation of the absorption coefficient.

We believe, however, that sparsity based non-linear algorithms are still promising and wish to evaluate next the algorithms based on convolutional sparse coding.

## ACKNOWLEDGEMENTS

The author would like to thank Prof. Kenji Nose Filho, who provided support and codes for the seismic blind deconvolution algorithms. This work was partially supported by the São Paulo Research Foundation

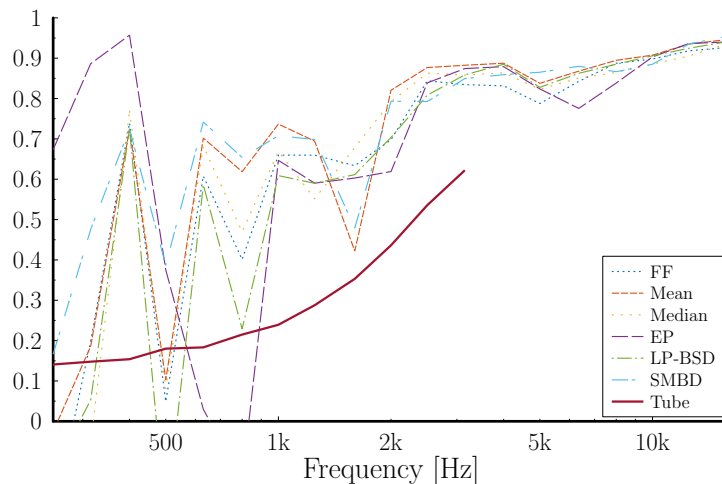


Figure 3. Comparison of absorption coefficient, averaged in third-octave bands, calculated with different pre-processing algorithms.

(FAPESP), grant #2017/08120-6 and the Brazilian National Council for Scientific and Technological Develop. (CNPq) under grant #400884/2016-0.

## REFERENCES

- [1] Kang J. Urban sound environment. Abingdon: Taylor & Francis; 2006.
- [2] Franssen EAM, van Dongen JEF, Ruysbroek JMH, Vos H, Stellato RK. NOISE ANNOYANCE AND PERCEIVED ENVIRONMENTAL QUALITY. INVENTORY 2003. *Epidemiology*. 2005 sep;16(5):S83.
- [3] Tzivian L, Dlugaj M, Winkler A, Weinmayr G, Hennig F, Fuks KB, et al. Long-Term Air Pollution and Traffic Noise Exposures and Mild Cognitive Impairment in Older Adults: A Cross-Sectional Analysis of the Heinz Nixdorf Recall Study. *Environmental Health Perspectives*. 2016 sep;124(9):1361–1368.
- [4] Eze IC, Foraster M, Schaffner E, Vienneau D, Héritier H, Pieren R, et al. Transportation noise exposure, noise annoyance and respiratory health in adults: A repeated-measures study. *Environment International*. 2018 dec;121:741–750.
- [5] Park SH, Lee PJ. Effects of indoor and outdoor noise on residents' annoyance and blood pressure. In: *EURONOISE 2018*. Crete; 2018. p. 435–441.
- [6] Brandão E, Lenzi A, Paul S. A review of the in situ impedance and sound absorption measurement techniques. *Acta Acustica united with Acustica*. 2015 may;101(3):443–463.
- [7] Londhe N, Rao MD, Blough JR. Application of the ISO 13472-1 in situ technique for measuring the acoustic absorption coefficient of grass and artificial turf surfaces. *Applied Acoustics*. 2009;70(1):129–141.
- [8] International Organization for Standardization. ISO 13472 — Measurement of sound absorption properties of road surfaces in situ — Part 2: Spot method for reflective surfaces; 2010.
- [9] Lacasta AM, Penaranda A, Cantalapiedra IR, Auguet C, Bures S, Urrestarazu M. Acoustic evaluation of modular greenery noise barriers. *Urban Forestry and Urban Greening*. 2016;20:172–179.
- [10] Bustamante FO. Método para medición in-situ del coeficiente de absorción acústica de materiales utilizando un solo micrófono y deconvolución regularizada. In: *XXIX SOMI - Congreso de Instrumentación*. Puerto Vallarta; 2014. .
- [11] Ducourneau J, Planeau V, Chatillon J, Nejade A. Measurement of sound absorption coefficients of flat surfaces in a workshop. *Applied Acoustics*. 2009;70(5):710–721.

- [12] Ottink M, Brunskog J, Jeong Ch, Fernandez-Grande E, Trojgaard P, Tiana-Roig E. In situ measurements of the oblique incidence sound absorption coefficient for finite sized absorbers. *The Journal of the Acoustical Society of America*. 2016 jan;139(1):41–52.
- [13] Richard A, Fernandez-grande E, Brunskog J, Jeong Ch. Impedance estimation of a finite absorber based on spherical array measurements. In: *Proc. 22nd International Congress on Acoustics*; 2016. .
- [14] Claerbout JF. *Fundamentals of geophysical data processing*. Blackwell; 1976.
- [15] Nose-Filho K, Romano MT. On  $\ell_p$ -norm sparse blind deconvolution. In: *IEEE International Workshop On Machine Learning For Signal Processing*, Reims, France; 2014.
- [16] Kazemi N, Sacchi MD. Sparse multichannel blind deconvolution. *Geophysics*. 2014;79(5):V143–V152.
- [17] Pais APTD, Malaguetta TC, Masiero BS, Bertoli SR. Comparison of in situ sound absorption measurements using single microphone and an array of microphones. In: *INTER-NOISE 2019, the 48th International Congress and Exposition on Noise Control Engineering*. Madrid, Spain; 2019. .
- [18] Vertatschitsch E, Haykin S. Nonredundant arrays. *Proceedings of the IEEE*. 1986;74(1):217–217.
- [19] Nascimento VH, Masiero BS, Ribeiro FP. Acoustic Imaging Using the Kronecker Array Transform. In: Coelho RF, Nascimento VH, de Queiroz RL, Romano JMT, Cavalcante CC, editors. *Signals and Images: Advances and Results in Speech, Estimation, Compression, Recognition, Filtering, and Processing*. CRC Press; 2015. p. 153–178.